Electrophoretic Migration of Submicron Polystyrene Latex Spheres in Solutions of Linear Polyacrylamide

Sergey P. Radko and Andreas Chrambach*

Section on Macromolecular Analysis, Laboratory of Cellular and Molecular Biophysics, National Institute of Child Health and Human Development, National Institutes of Health, Bethesda, Maryland 20892-1580

Received September 11, 1998

ABSTRACT: The electrophoretic migration of highly cross-linked carboxylated polystyrene latex spheres of 55, 140, and 215 nm radius (R) in solutions of linear polyacrylamide of 0.4×10^6, 0.6×10^6, and 1×10^6 molecular weight, in the 0.1−1% concentration range, was studied by capillary zone electrophoresis. The electric field strengths applied ranged from 40 to 530 V/cm. At the ionic strength used, these particles must be considered "large", exhibiting $\kappa R \geq 13$ where κ^{-1} is the thickness of electric double layer. In the semidilute polymer concentration regime, the radius of the particles severalfold exceeds the average mesh size, ξ, in the polymer network. It was found that particle retardation (expressed as μ/μ_0 where μ and μ_0 are particle electrophoretic mobilities in polymer solution and buffer alone) at a given polymer concentration decreases with both increasing particle size and electric field strength but increases with polymer molecular weight. The dependence of retardation on polymer concentration, c, follows a "stretched exponent", $\mu/\mu_0 = \exp(-\alpha c^{\upsilon})$. The prefactor α and the exponent υ are particle radius and electric field strength dependent. The microviscosity of polymer solutions defined as μ_0/μ was well below values of zero shear viscosity measured viscometrically even when no dependence of microviscosity on electric field strength was observed. These findings were interpreted in terms of (i) a local shearlike deformation of the polymer network upon particle passage, resulting in a progressive decrease of the network entanglement density at the particle locales with particle translational velocity and, thus, a decrease of network resistance to particle penetration; and (ii) a progressive polymer depletion near the particle surface, with increasing particle radius at the scale of R/ξ, which facilitates electrophoretic migration of the microparticle in the polymer solutions.

Introduction

The size-dependent electrophoretic separation ("sieving") of macromolecules in polymeric media such as gels has been known for decades.[1] Recently, buffered solutions of neutral polymers, mostly in the semidilute concentration regime, have attracted a great deal of interest as electrophoretic media both for analytical[2,3] and preparative[4] size separations. This interest was primarily due to the spread of capillary electrophoresis, since polymer solutions have demonstrated a number of technical advantages over gels in that particular technique.[5] Although efforts centered on the sieving of flexible linear DNA species,[2,3] the polymer solutions, due to unlimited penetration by rigid particles in contrast to gels, also provide a medium for the size-dependent electrophoretic separation of particles in the submicron or micron size range ("microparticles").[6] Despite the practical importance of such separations, very little is known concerning the mechanisms by which polymer solutions exert their sieving effects on the microparticles.

The transport through polymer solutions of spherical rigid microparticles of different origin, ranging in diameter from tens of nanometers to several micrometers, was extensively studied over the past two decades. However, the main focus was on the particle diffusion in those media. (A comprehensive list of references on this subject may be found, for example, in the recent publications of Gold et al.[7]) Also, a number of studies on the particle transport through polymer solutions in centrifugal fields were carried out for both theoretical[8,9] and practical[10] purposes. (See ref 9 for more references on this subject.) The electrophoretic migration of particles in solutions of neutral polymers, mostly in the dilute concentration regime, was also a subject of theoretical and experimental investigations over the past decades but mostly for purposes of electrokinetic measurements rather than the size-dependent separation of particles (reviewed recently in ref 11).

The electrophoretic motion of charged particles is distinguished from the diffusive motion or the motion induced by a centrifugal force by a different composition of forces acting on the particle. In an electrolyte solution, a charged particle is known to be surrounded by the ionic atmosphere which forms the so-called electric double layer (EDL).[12] When the distortion of that atmosphere by the imposed electric field or by the Brownian motion of the particle may be neglected, the particle's steady translational motion in a viscous medium results from the balance of three forces: the driving force exerted by the dc field on the particle due to its electrokinetic charge ($\mathbf{F}_1$), the Stokes drag ($\mathbf{F}_2$), and an "additional" hydrodynamic force, the electrophoretic retardation force ($\mathbf{F}_3$), arising from the electrophoretic motion of counterions in the diffusive periphery of the EDL.[12,13] The ratio between the "drag" forces is of the order of κR ($|\mathbf{F}_3|/|\mathbf{F}_2| \approx \kappa R$), where κ^{-1} is the Debye length (the electric double-layer thickness) and R the particle radius.[13] Thus, the force $\mathbf{F}_1$ applied to small particles (relative to κ^{-1}) is compensated for mainly by the "ordinary" hydrodynamic resistance of the medium $\mathbf{F}_2$ (the Stokes viscous drag), while for large ones it is compensated for mainly by the electrophoretic retardation force $\mathbf{F}_3$. In the latter case, the fluid is at rest outside of the EDL, and all drag is due to viscous tensions on the particle surface caused by the electro-

* To whom correspondence should be addressed. FAX 301-402-0263; e-mail acc@cu.nih.gov.

10.1021/ma9814447
Published on Web 03/25/1999

osmotic slipping of the fluid. It can be expected that when $\kappa R \sim 1$, all three forces will be of the same order.[13]

For an arbitrary value of κR, the electrophoretic mobility, μ, of a rigid nonconducting spherical particle, moving in a medium of viscosity η is known to be given as[12,13]

$$\mu = (2\epsilon\zeta/3\eta)f(\kappa R) \quad (1)$$

where ϵ is the dielectric permittivity of the medium and ζ the particle's zeta potential. $f(\kappa R)$ is Henry's function which ranges from 1 at $\kappa R \ll 1$ (the Hückel limit) to 1.5 at $\kappa R \gg 1$ (the Smoluchowski limit). One of the assumptions underlying eq 1 is that the viscous medium is a continuum characterized by uniform ϵ and η. The presence of neutral polymers at moderate concentrations is known not to alter the dielectric permittivity of the medium to any appreciable extent (ref 14 and references therein). Therefore, the condition of uniformity of ϵ seems obeyed. Yet, the situation regarding the viscosity of the medium is obviously different.

The particle will face the medium as a "viscous continuum" if its size is much greater than the characteristic size of the structural inhomogeneities of the medium. In dilute polymer solutions where polymer coils are separated in space, that characteristic size would be the mean radius of gyration, R_g, of the coils. When the polymer concentration increases, at some point (the so-called entanglement threshold, c^*), the polymer coils start to overlap and to penetrate into each other, forming a continuous spatial network due to steric interactions of polymer chains ("entanglements").[15] Polymer solutions at concentrations above c^*, known as semidilute, are characterized by a screening length, ξ, which may be conceived as the average distance between points of entanglement or as the average size of mesh in the transient polymer network.[15] Thus, the solution of polymers would present itself as a continuum in relation to the spherical particle if R is much greater than R_g or ξ in the dilute and semidilute concentration regimes, respectively. Yet, a polymer solution in the concentration range exceeding its coil overlap concentration, c^*, by no more than a few times will have a screening length, ξ, of the order of the radius of gyration of the coil, R_g, which may easily be a few tens of nanometers. That can lead to a failure of the condition of a continuum for a microparticle of an arbitrary size in the polymeric medium. That point has been recognized from early on.[16] The frictional force experienced by the particle can no more be expected to be directly proportional to the bulk viscosity of the solution. To maintain validity of eq 1, one may describe the viscous friction in terms of microviscosity (microscopic or local viscosity) which, as defined by Lin and Phillies,[17,18] reflects properties of the medium over a distance commensurate with the size of the microparticle. From eq 1, the microviscosity, η_μ, can be measured as

$$\eta_\mu/\eta_0 = \mu_0/\mu \quad (2)$$

where η_0 is a solvent (buffer) viscosity, and μ_0 and μ the electrophoretic mobilities of the particle in the absence and presence of polymers, respectively. Equation 2 assumes that the electrostatic properties of the medium are not affected by the presence of neutral polymers.

However, in the case of electrophoretic migration, further characteristic dimensions of the polymer medium need to be considered: In the vicinity of a solid−liquid interface, the properties of polymer solutions can be strongly modified relative to those in the bulk phase. That occurs if there exists a nonuniform monomer concentration profile near the solid surface due to an interaction between polymer, solvent, and particle surface.[19,20] Therefore, on one hand, one may assume that a particle suspended in the polymer solution might be surrounded by a region of a characteristic thickness λ where viscosity differs from that of the bulk solution. On the other hand, for particles whose radii greatly exceed the thickness of the electric double layer, κ^{-1}, the dominant drag force would be that due to the viscous friction within that layer. If λ is commensurate with or exceeds κ^{-1}, the drag experienced by the particle may be considerably different from that expected according to the bulk viscosity (eq 1) even when $R \gg R_g$ (or ξ). Thus, the condition of "viscous continuum" must be augmented by that of $\kappa^{-1} \gg \lambda$. For $\lambda \geq \kappa^{-1}$, the concept of microviscosity, now reflecting the properties of the medium within the EDL, may be applied.

Uniformity of viscosity in eq 1 implies as well that the medium is a Newtonian fluid whose viscosity is not affected by the gradient of the fluid velocity field surrounding the moving particle. Yet, polymer solutions are known to belong to the opposite class of fluids, the non-Newtonian ones.[21,22] Even if all the conditions for a "continuum" are obeyed, a value of viscosity in eq 1 may correspond, in fact, to that at some finite shear rate characterizing the local shear due to flow of the "macromolecular fluid" corresponding to the translational motion of the particle. Similarly to the macroscopic viscosity, the microviscosity is also likely to depend on the fluid velocity field around the particle.

The present study reports experimental findings for spherical rigid microparticles of 0.11−0.43 μm diameter subjected to electrophoresis at various field strengths in buffered solutions of linear polyacrylamide of different molecular weight and known viscosity, with the purpose of gaining some insight into the physical mechanisms that underlie the microviscosity of the polymer solution and govern the size-dependent electrophoretic migration of microparticles in polymeric media.

Experimental Section

Materials. The electrophoretic buffer was a solution of 22 mM Tris, 22 mM boric acid, and 0.5 mM Na_2EDTA (designated TB buffer), prepared by diluting a 40X concentrate (0.89 M Tris, 0.89 M boric acid, 0.02 M Na_2EDTA, pH 8.3, BioWhittaker, Inc., Walkersville MD, Cat. No. 16-012BN).

Particles were fluorescent carboxylate modified polystyrene latex spheres of 110 ± 5, 280 ± 7, and 430 ± 12 nm diameter (Interfacial Dynamics Corp., Portland, OR, Cat. No. 2-FY-100,1; 2-FY-300,1; 2-FY-400,1; designated as PS-55, -140, and -215, respectively). Particles were supplied as 2% solid latex suspensions in distilled water. The suspensions were appropriately diluted to obtain samples of 0.002, 0.006, 0.02, 0.06, and 0.2% solids in TB buffer for particles of each size. These sample concentrations correspond to particle volume fractions of 1.9×10^{-5}, 5.7×10^{-5}, 1.9×10^{-4}, 5.7×10^{-4}, and 1.9×10^{-3}, respectively (based on polystyrene latex density of 1.05 g/mL).

Polymers were linear polyacrylamide (PA) of different molecular weight. Solid PA of nominal molecular weight (M_r) of 400 000 and 600 000 with polydispersity (M_w/M_n) of 2.6 and 2.5, respectively, was obtained from Polysciences, Inc. (Warrington PA, Cat. No. 19790, 18259; designated as PA-0.4 and PA-0.6, respectively). Their 1.5% (w/v) aqueous stock solutions were prepared by solubilization in deionized water with gentle shaking overnight. PA of M_r 700 000−1 000 000 and unknown

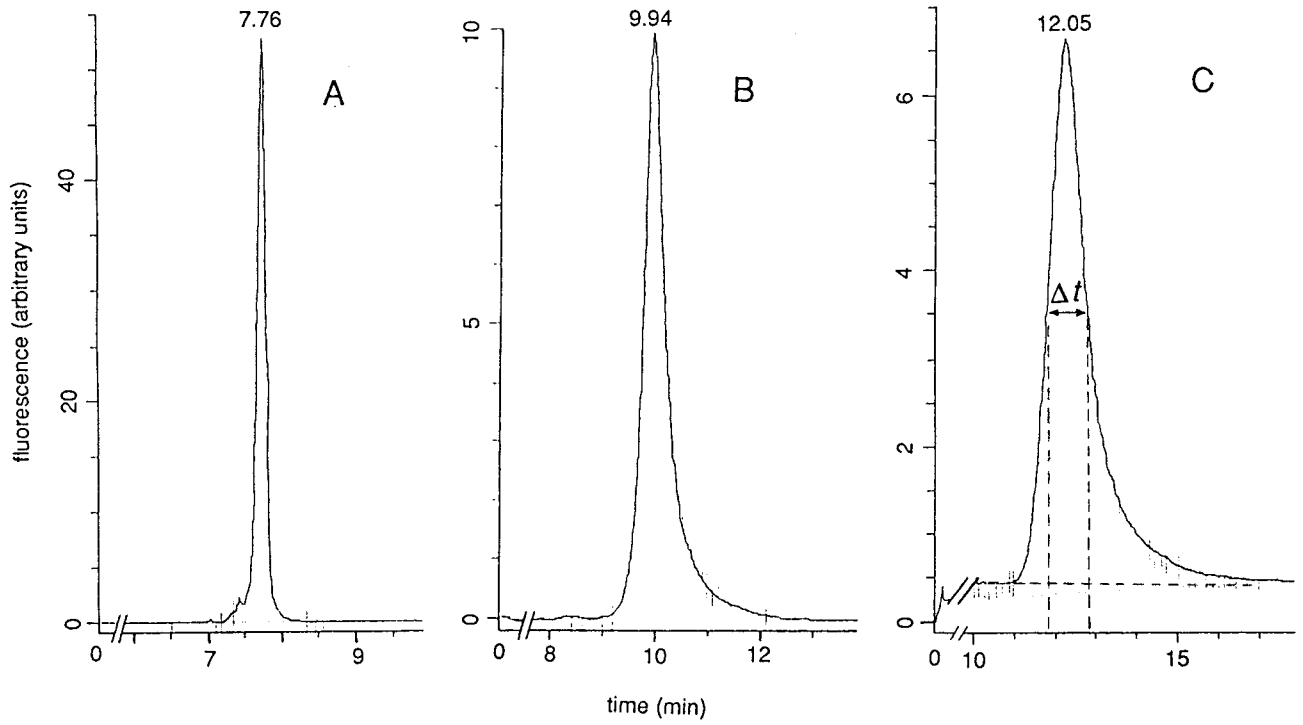

Figure 1. Representative electropherograms. The 280 nm diameter polystyrene latex spheres, sample concentration 0.02% solid latex. CZE: 150 μm i.d. capillary, 40 cm effective capillary length, 270 V/cm, 25 °C, sample volume injected ≈0.1 μL. Panel A, TB buffer alone; panel B, 0.5% PA-1 solution in TB buffer; panel C, 1.0% PA-1 solution in TB buffer.

polydispersity (Polysciences, Cat. No. 19901; designated as PA-1) was supplied as a 10% aqueous solution. Aqueous PA solutions were appropriately mixed with the buffer concentrate to obtain the required PA concentrations within the range 0.1%−1.0% in TB buffer.

For convenience, a dimensionless polymer concentration, polymer weight fraction (gg^{-1}), was used in all calculations unless stated otherwise.

Methods. *(A) Electrophoresis.* Electrophoretic mobility of the particles was measured by capillary zone electrophoresis (CZE). The capillary electrophoresis apparatus used (P/ACE 2100, Beckman Instruments, Fullerton, CA) was equipped with a fluorescence detector and temperature control. Capillaries were fused silica tubing of 47 cm length, 150 μm i.d., and 360 μm o.d., externally coated with polyamide (Polymicro Technologies, Inc., Phoenix, AZ, Cat. No. TSP150375). The detection window was formed at 40 cm from the injection (cathodic) end of the capillary (effective capillary length), using a glowing wire to remove the external coating. Thereafter, the capillaries were internally coated with 3% un-cross-linked polyacrylamide to suppress the electroosmotic flow.[23] Capillaries were tested with regard to electroosmosis prior and after CZE by determining the mobility of picric acid, 2.8×10^{-4} $cm^2/(s\ V)$ (J. T. Baker, Inc., Phillipsburg, NJ, Cat. No. 0276-01). Capillaries exhibiting a picric acid mobility of less than 2.7×10^{-4} $cm^2/(s\ V)$ were discarded. CZE was conducted at 25 °C as described elsewhere,[24] using PA solutions in TB buffer. Sample injection by pressure (3.5 kPa) was carried out taking into account the dependence of injection time on viscosity of the polymer solution as follows. Polymer solution containing a dye (SPADNS, Aldrich Chemical Co., Cat. No. 11,475-8) was pressure (3.5 kPa) injected into the capillary filled with the same solution without dye. The time required by the dye to reach the detector in polymer solution (t_p) and buffer (t_o) was measured. The ratio of t_p/t_o was used to calculate the injection time in the presence of polymer providing a constant injection volume independent of polymer concentration. In free buffer, the injection time used was 1 s, the minimum tolerated by the instrument. That injection volume corresponded to a starting zone not exceeding 2% of the effective capillary length.

(B) Viscometry. Viscosity measurements were carried out by means of a rotational viscometer equipped with a digital display (model DV-I+, Brookfield Engineering Labs, Inc., Stoughton, MA), using the Brookfield UL cylindrical adapter providing shear rates of 0.6−122 s^{-1}. The viscometer tube assembly was immersed in a thermostated bath at 25 °C.

(C) Conductivity Measurements. Electric conductivity of the electrophoretic buffer was measured at various temperatures by conductivity meter (model CDM 2d, Radiometer, Copenhagen, Denmark).

Data Processing. Electrophoretic mobility of the particles was provided by the P/ACE 2100 software (Beckman, SYSTEM GOLD), based on the migration time, t_m, corresponding to the mode of the fluorescence distribution (as illustrated by Figure 1). The peak width at half-height, Δt, marked by the double arrow in Figure 1C, was obtained by using the "zoomed" graphic output provided by SYSTEM GOLD software. To take into account the peak broadening due to differences in particle mobility, the peak width, Δt, was divided by the peak migration time, t_m, giving the relative peak width, $\Delta_{1/2} = \Delta t/t_m$.

For PA-1, measured values of absolute viscosity (η, cP) were used to calculate specific ($\eta_{sp} = (\eta_{solution} - \eta_{solvent})/\eta_{solvent}$), reduced ($\eta_{sp}/c$), and inherent ($\ln[\eta_{solution}/\eta_{solvent}]/c$) viscosities, where c is the polymer concentration (g/mL). Using average values of viscosity within the shear rate range of 6.1−61 s^{-1} (Figure 2), the intrinsic viscosity, $[\eta]$, was obtained by a linear extrapolation of plots, comprising the values of reduced and inherent viscosities at low PA concentrations, to infinite dilution. From $[\eta]$, the molecular weight of the polymer was derived by use of the Mark−Houwink−Sakurada (MHS) equation, $[\eta] = KM_r^a$, where $a = 0.8$ and $K = 4.9 \times 10^{-3}$ mL/g for aqueous PA solutions at 25 °C.[25]

The best-fit data analysis was carried out by using program SIGMAPLOT (Jandel Scientific, Corte Madera, CA).

Results

The relation between viscosity of PA-1 in TB buffer at 25 °C and polymer concentration is depicted in Figure 2. The linear extrapolation to zero PA concentration of both the reduced and inherent viscosities (see above) yielded values of $[\eta]$ of 299 ± 16 and 313 ± 6 mL/g,

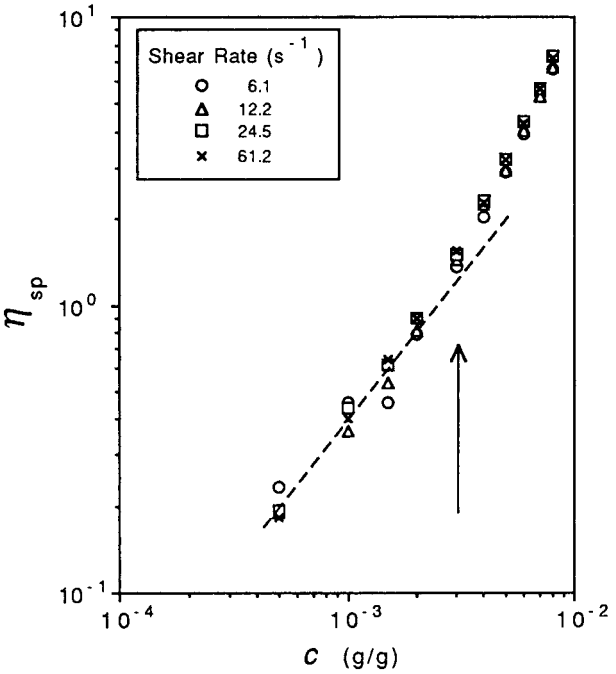

Figure 2. Specific viscosity of PA-1 solutions at 25 °C, measured at various shear rates, vs polymer concentration.

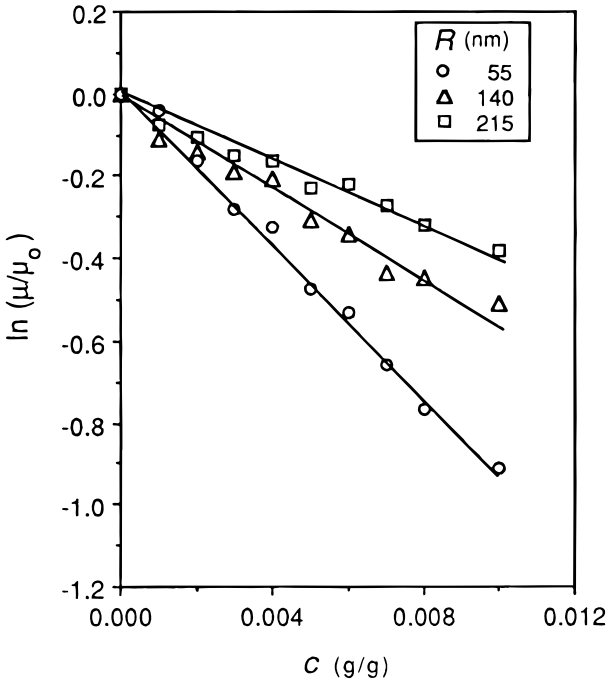

Figure 3. Representative plots of relative mobilities vs PA-1 concentrations for polystyrene spheres of various sizes. CZE conditions and latex concentration as in Figure 1. Straight lines are drawn to guide the eye.

respectively. The mean value, 306 mL/g, was used for further computations. As evidenced by the rheological measurements, the values of solution viscosity are independent of shear rates within the range of 6.1−61 s^{-1} (Figure 2) and may be considered to be those at zero shear rate. Therefore, the intrinsic viscosity obtained by using those values is that at the zero shear rate and may be applied to calculate both the entanglement threshold, c^*, and the PA molecular weight.

The literature presents several ways to estimate c^*. Values for c^* can be calculated from $1/[\eta]$[7,26,27] or from $3M_r/(4\pi N_A R_g^3)$,[7,28] where N_A is Avogadro's number. The latter expression may be rewritten as $1.5/[\eta]$.[2] Values of c^* were also determined as the concentration at which the double-logarithmic plot of specific viscosity vs polymer concentration departs from linearity (slope = 1).[29] Such is supposed to correspond to a progressive transition of the polymer solution into the entangled state.[29,30] Since the value of c^* estimated from $1/[\eta]$ was 0.0033 gg^{-1}, close to that obtained by such departure (Figure 2), that value was taken to pinpoint the cross-over from dilute to semidilute concentration regimes in PA-1 solutions.

The PA-1 molecular weight was derived from the intrinsic viscosity as 1×10^6 using the MHS equation. It should be noted that the viscosity-average molecular weight may differ from that obtained by size-exclusion chromatography and specified by the manufacturer.

In Figure 3, representative semilog plots of particle relative mobility, μ/μ_0, vs PA concentration, c, are shown. The best-fit analysis shows that μ/μ_0 is a stretched exponential function of c,

$$\mu/\mu_0 = \exp(-\alpha c^{\upsilon}) \tag{3}$$

Both the constant α and the scaling exponent υ were found to depend on parameters of the system such as particle size and concentration, polymer molecular weight, and strength of the applied electric field. At the arbitrarily chosen electric field strength, 270 V/cm, the exponent υ was independent of particle concentration within the limits of experimental scatter and error and slightly depended on particle size (Table 1). By using average values of the exponent ($\bar{\upsilon}$, Table 1), the parameter α was analyzed as a function of particle concentration. It was found that α decreases near-linearly with $\Phi^{1/3}$, where Φ is the particle volume fraction (Figure 4). At a given particle concentration, α shows a decline with particle radius within the range of 55−215 nm. The electrophoretic mobilities of PS-140 and -215 in buffer alone did not demonstrate any appreciable change with particle concentration. Thus, the decrease in coefficient α with Φ (Figure 4) is due to the increase in the mobility, μ, of the particles at a given polymer concentration and not to a decrease in the free mobility μ_0. For PS-55, a monotonic decrease in values of μ_0 with Φ of about 6% was observed over the particle concentration range studied. Thus, the decline in α with Φ for PS-55 is by one-half due to a change in particle free mobility.

Table 1. Scaling Exponent υ of Eq 3 at Various Sample Concentrations (Polystyrene Latex Volume Fractions): Best Fits of the Data of Figure 3 to Eq 3 for All Polystyrene Latex Concentrations Used; Exponent υ Was Computed Using Program SIGMAPLOT (Jandel Scientific, Corte Madera, CA)

	particle volume fraction (v/v), $\times 10^{-5}$					
particle radius (nm)	1.9	5.7	19	57	190	$\bar{\upsilon}$
55	1.10 ± 0.08	1.06 ± 0.07	1.07 ± 0.07	1.11 ± 0.08	1.06 ± 0.08	1.08
140	0.9 0 ± 0.09	0.85 ± 0.07	0.86 ± 0.08	0.85 ± 0.08	1.04 ± 0.08	0.90
215	0.97 ± 0.08	0.91 ± 0.10	0.83 ± 0.13	0.81 ± 0.08	0.99 ± 0.07	0.90

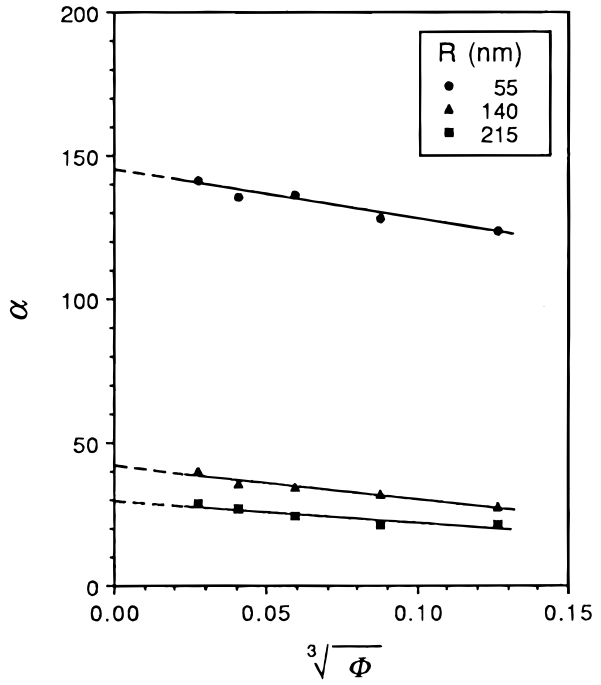

Figure 4. Prefactor α of eq 3 for particles of various radii vs polystyrene latex volume fraction Φ. Prefactor α was calculated by the best fit of eq 3 to the experimental data for $v = \bar{v}$ (Table 1). CZE conditions as in Figure 1.

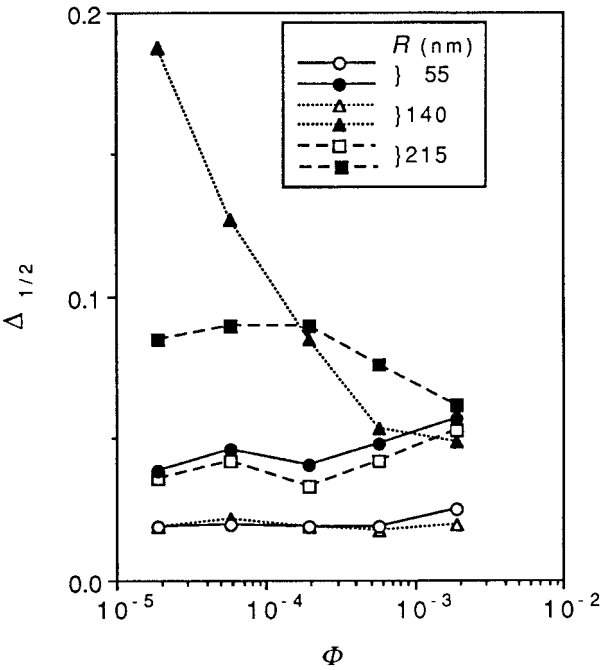

Figure 5. Relative peak width for polystyrene spheres of various sizes vs polystyrene latex volume fraction Φ. Open symbols correspond to CZE in TB buffer alone; closed symbols correspond to CZE in 1% PA-1 solution in TB buffer. CZE conditions as in Figure 1.

As seen in Figure 5, the relative peak width, $\Delta_{1/2}$, does not change appreciably with particle concentration for PS-55 and -140 but demonstrates a moderate increase for PS-215 with Φ above $\Phi \approx 0.0002$. In the 1% PA-1 solution, $\Delta_{1/2}$ exhibits more complex behavior, slightly increasing and decreasing for PS-55 and -215, respectively, with Φ above $\Phi \approx 0.0002$, while decreasing substantially for PS-140 over the range of the particle concentrations used (Figure 5).

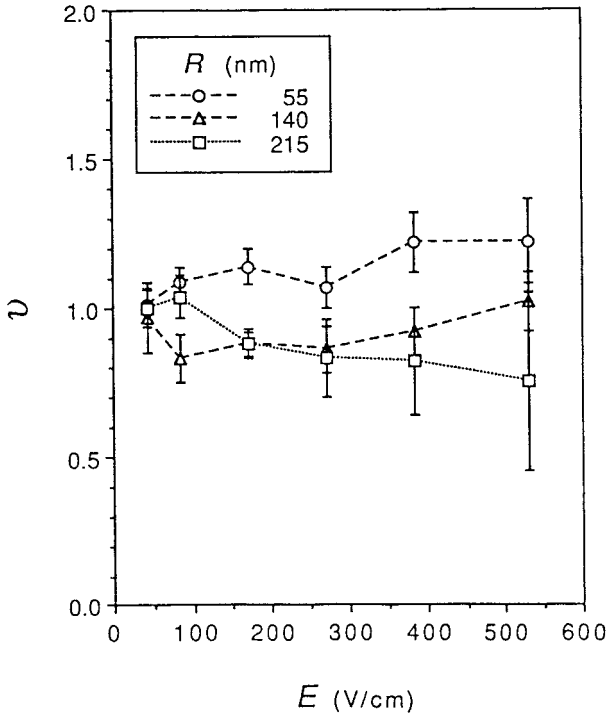

Figure 6. Exponent v of eq 3 for particles of various radii vs applied electric field strength. Values of exponent v were obtained by the best fit of eq 3 to the experimental data. Particle concentration and CZE conditions as in Figure 1 except for the field strength.

When plotted against electric field strength, the scaling exponent varies differently for the particles of different size in the range of field strengths investigated (43−530 V/cm) at the given particle concentration of 0.02% solids (Figure 6). Despite the experimental scatter, v shows a clear trend to increase with field strength for the particle of 55 nm radius, and the opposite trend when the particle radius increases to 215 nm. To analyze retardation by the polymeric matrix of the particles of different size as a function of field strength, E, the experimental data were best-fitted to a single exponential form:

$$\mu/\mu_0 = \exp(-\alpha' c) \qquad (4)$$

As seen in Figure 6, such an approximation is justified at low values of field strength. Although the scaling exponents diverge from each other for PS-55 and PS-215 with increasing E, the range of v values within the standard errors still includes the value $v = 1$ and, thus, allows for the approximation by a single exponent throughout the range of field strengths used.

Figure 7 shows the parameter α′ plotted against electric field strength, E. For all particles, retardation was found to weaken with increasing E. At a given field strength, smaller particles were retarded more strongly by the polymeric matrix than large ones. Electrophoresis is known to be always accompanied by Joule heating. At high electric fields, it can result in an appreciable increase in temperature of the electrophoretic medium despite the effective heat dissipating capacity of thin capillaries. Since the viscosity of polymer solutions is known to decrease with temperature,[21,22] the temperature increase due to Joule heating must be analyzed as a potential source of the observed decline in retardation with E (Figure 7). As seen from Figure 8, the capillary conductance did not exhibit any appreciable increase

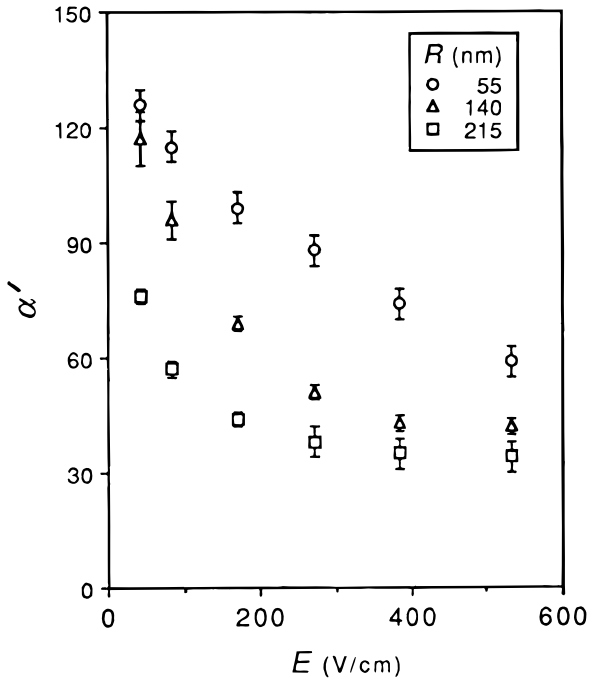

Figure 7. Parameter α′ of eq 4 plotted against applied electric field strength. Values of α′ for polystyrene spheres of various sizes were calculated by the best fit of eq 4 to the experimental data. Particle concentration and CZE conditions as in Figure 1 except for the field strength.

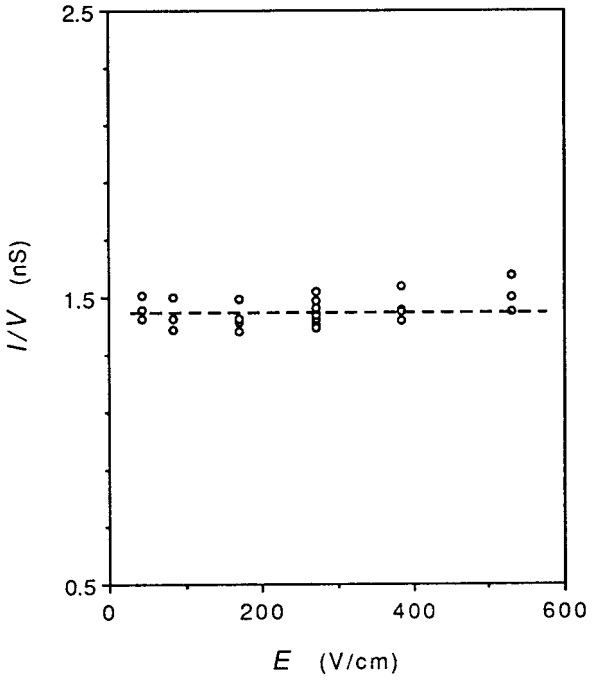

Figure 8. Conductance in a capillary filled with TB buffer vs applied electric field strength. CZE conditions as in Figure 1 except for the field strength.

throughout the range of E used: the increase of about 3% was observed only at the highest field strength, 530 V/cm. The measurement of the conductivity of the TB buffer as a function of temperature has shown that its conductivity increases about 10% in the range 25−30 °C, i.e., 2%/°C, at an average. Hence, the average temperature increase inside the capillary would not exceed 1−2 °C even at 530 V/cm. The absolute viscosities of PA-1 solution measured in the same temperature range have demonstrated an overall decrease of about

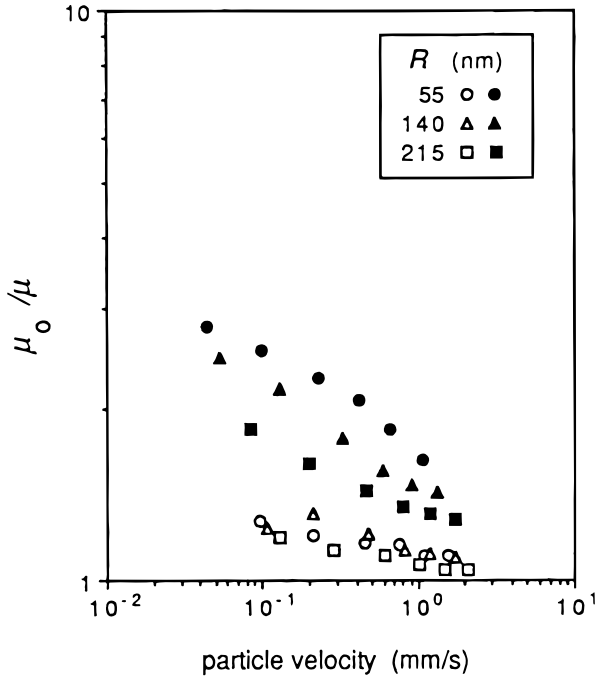

Figure 9. Microviscosity, defined as μ_0/μ, of 0.2% (open symbols) and 0.8% (closed symbols) PA-1 solutions as a function of particle translational velocity for particles of various radii. Particle concentration and CZE conditions as in Figure 1 except for the electric field strength.

8%. Thus, one may expect macroscopic viscosity changes inside the capillary due to Joule heating of not more than 2%−3%. It seems unlikely that microscopic viscosity would decrease with temperature by more than an order of magnitude faster than the macroscopic one. Therefore, the observed reduction in particle retardation by a factor of 2 with E (Figure 7) cannot be accounted for by Joule heating.

In Figure 9, relative microviscosities of polymer solutions measured as μ_0/μ (eq 2) are plotted versus the velocity of the translational motion of the particle, $v = \mu E$. Microviscosity decreases monotonically with particle velocity in both the dilute and semidilute concentration regimes (Figure 9). In the dilute regime ($c = 0.002$ gg^{-1}), there is no clear dependence of μ_0/μ on particle size within the limits of experimental scatter, whereas in the semidilute regime ($c = 0.008$) a decline in microviscosity with particle radius, R, at a given v, is clearly demonstrated.

Figure 10A,B,C depicts the microviscosity of a 1% solution of PA of different molecular weights vs particle velocity for PS-55, -140, and -215, respectively. By application of the MHS equation, we calculated $[\eta] = 0.0049M_r^{0.8}$ (see Experimental Section). Estimating c^* as $1/[\eta]$, these solutions can be shown to be semidilute. All PA solutions studied demonstrate the same pattern, *viz.* a decline in microviscosity with particle velocity, though the rate of decline differs for different particles and PA sizes. Thus, for PA-0.4 and PS-215 no appreciable dependence on v was observed. At a given particle velocity, microviscosity increases with M_r for each particle as well as decreases with particle radius for PA of each molecular weight studied.

Discussion

Scaling Behavior. Theoretical models that describe the transport of rigid spherical particles in polymeric

media which are, to some extent, relevant to the present study were proposed by Rodbard and Chrambach,[31] Ogston et al.,[32] Langevin and Rondelez,[8] Altenberger and Tirrel,[33] and Cukier.[34] The models use very different assumptions as to the physical forces retarding particle motion in a polymeric medium. However, all models link the retardation factor, f_0/f (where f_0 is the frictional force experienced by the particle in a pure solvent and f that in a polymeric medium), to a concentration-dependent parameter, d, and the particle radius, R, in the form like

$$f_0/f = \exp[-(R/d)^{\delta}] \tag{5}$$

Here $d \sim c^{-\upsilon}$ and represents a characteristic distance in the polymeric medium; δ and υ are scaling exponents. In terms of microviscosity, $f_0/f \equiv \eta_0/\eta_\mu$.

Rationales leading to d, δ, and υ are different in different models. Rodbard and Chrambach have employed a purely geometric approach based on previous work of Ogston[35] and Giddings et al.[36] They considered the retardation factor to be proportional to a fractional volume available to a spherical particle in a random suspension of rigid inert geometric obstacles and arrived for fibers at the following expression:

$$f_0/f = \exp(-K_R c) \tag{6}$$

where $K_R \sim R^2$ is the so-called retardation coefficient. The model was shown to adequately describe the retardation of nondenatured proteins in cross-linked gels[1,31] and was widely applied in electrophoresis over the past decades.[1−3,5,29,30] Recently, Slater and coworkers taking into account the percolation pathways and the more detailed architecture of the gel have shown in a number of publications (ref 37 and references therein) that the fractional volume should be described by a series expansion rather than by the single-exponential form of eq 6. Langevin and Rondelez presented a model based on the scaling argument, in which $d \equiv \xi$ and δ is limited by the value of 2.5 (in the case of fixed entanglement points, i.e., a gel).[8] When the entanglements are not fixed (a semidilute solution), the exponent is suggested to be smaller. The authors claim that the model rests on an estimate of the entropy reduction of a single mesh unit with original size ξ when it is extended to size R. When $R/\xi \to \infty$, f_0/f is expected to approach η_0/η. The calculation of Ogston et al.[32] considers the placement of obstacles blocking the particle's path. To be able to move forward, the spherical particle has to fit through the gaps in a network of randomly placed rigid rods. The calculation resulted in an expression of the form of eq 6 with $\delta = 1$ and $\upsilon = 1/2$. By contrast, Cukier[34] and Altenberger and Tirrel[33] treat particle retardation in a polymeric medium as a result of hydrodynamic interactions between the spherical particle and externally fixed pointlike obstacles. Physical collisions (nonhydrodynamic interactions) between the particle and the polymer chains are not included in those models. The concentration regimes considered by the models are different: while Altenberger and Tirrel considered a limiting case of $c \to 0$, the model of Cukier deals with semidilute solutions. Altenberger and Tirrell predict[33] $f_0/f = 1 - Ac^{0.5} - Bc^1$, where A and B are functions of R; A is directly proportional to the particle radius. Cukier[34] gives an expression for the retardation factor in the form of eq 6 with $\delta = 1$; d designates a characteristic length of the hydrodynamic screening. In accordance with deGennes' assertion[15] that the polymer hydrodynamic and screening lengths share the same dependence on concentration, and since[15] $\xi \sim c^{-3/4}$ for a semidilute solution of flexible linear polymers, one may write $d \sim c^{-3/4}$ ($\upsilon = 3/4$). It should be pointed out that all the models employing the screening length imply that the retardation factor is independent of polymer molecular weight, since $\xi \neq f(M_r)$.[15]

It is important to note that, to adapt the hydrodynamic models to electrophoretic migration of particles in polymer solutions, the electrophoretic retardation force must not be dominant. This implies that the thickness of the electric double layer, κ^{-1}, surrounding the particle has to exceed or, at least, to be commensurate with, particle radius. Since κ^{-1} is known to have values of several nanometers at the ionic strengths usually used in electrophoretic buffers,[12] this condition is thought to hold in the macromolecular size range (roughly 2−15 nm in diameter).

Using semidilute solutions of poly(ethylene glycol) (PEG) as a polymeric matrix in electrophoresis, the retardation factor for five protein particles ranging in size from 2 to 5 nm radius was found to be given by eq 5 with scaling exponents δ and υ of 1 and 0.69, respectively.[38] The retardation was found to be nearly independent of polymer M_r ($\ln f_0/f \sim M_r^{0.04}$) and independent of the electric field applied (from 40 to 400 V/cm). This result is similar to that of Langevin and Rondelez, obtained by ultracentrifugation for various spherical particles with 2.5−17.5 nm radius in semidilute PEG solutions, viz. $\delta = 1$, $\upsilon \cong 0.62$, and a retardation factor independent of polymer M_r.[8] The study by Phillies[39] showing that the diffusion coefficient of bovine serum albumin in PEG solutions depends on the polymer molecular weight does not contradict these results because the author used dilute rather than semidilute PEG solutions. (The highest concentrations of PEG were 0.5% and 0.25% for M_r 1×10^5 and 3×10^5, respectively.) In the dilute concentration regime, protein electrophoretic migration was also found by the authors to depend on polymer molecular weight.[40] The transition from the dilute to the entangled solution is also likely to be a source of the increase in retarding capacity of dextran with molecular weight, as observed by Laurent and Persson in one of the first studies on protein transport in polymer solutions.[41] In the concentration range used, 0.5%−3.5%, the increase was most marked at the lower molecular weights (10^4 and 8×10^4), while the difference between dextrans of M_r of 5×10^5 to $(2.5-5) \times 10^7$ was found to be relatively small.

Thus, the theoretical model of Langevin and Rondelez and that of Cukier seem to adequately describe the major features of particle retardation, as experimentally observed in the semidilute solution of neutral flexible polymers, when the particle size range is commensurate with, or less than, the average size of a mesh unit in the polymer network. It holds up to a particle size of about 15 nm in radius as demonstrated by retardation of polystyrene latex nanospheres subjected to electrophoresis in semidilute solutions of linear polyacrylamide (5×10^6 M_r, 0.1%−0.8% concentration range).[42] Above that size range, the retardation of their electrophoretic migration becomes polymer molecular weight and electric field strength dependent.

As shown in the present study, the retardation of submicron-sized particles can still be described by a

stretched exponent (Figures 3 and 6 and Table 1), although with both the constant α and the scaling exponent v (eq 3) being electric field strength dependent. Yet, the applicability of eq 3 to such a wide particle size range demonstrates the power of that function to fit a monotonic experimental dependence rather than its relevance to the models considered above. The irrelevance of eq 3 to the theoretical model, in the range of particle sizes under study, may be understood when one compares the characteristic polymer lengths with the size of the particles, as follows. The radius of gyration of a polymer coil, R_g, may be calculated as

$$R_g = 0.4([\eta]M_r/\Phi_F)^{1/3} \quad (7)$$

where Φ_F is the Flory constant; $\Phi_F = 2.3 \times 10^{23}$ mol^{-1} for a good solvent.[22] For PA-1, it gives $R_g = 44$ nm. Since[28]

$$\xi = 0.5R_g(c/c^*)^{-0.75} \quad (8)$$

the values of the screening length ranges from 22 to 9 nm with c (from 0.003 gg^{-1} ($=c^*$) to 0.01 gg^{-1}, the highest PA concentration used). Recently, the relation between ξ and PA concentration in the semidilute regime has been obtained by small-angle neutron scattering as[43]

$$\xi\,(\text{nm}) = 0.21c^{-0.76} \quad (9)$$

with c in g mL^{-1}. Equation 9 provides values of 17−7 nm for ξ in the same concentration range, in good agreement with those derived from eq 8. For PS-55, -140, and -215, the ratio of R/ξ will lie in the ranges 3−8, 8−20, and 13−31, respectively. Thus, the particle cannot anymore be imaged as a "fish" moving through a "fishnet", a mnemonic image implied in all theoretical models mentioned above, once the mesh size of this "fishnet" becomes too fine.

It is not clear from the available data how the transition from the dilute to the semidilute concentration regimes at $c^* \approx 0.003$ gg^{-1} affects the parameters of the stretched exponent in eq 3. Though no breaks on the experimental curves were observed at this concentration (Figure 3), the experimental data do not suffice to rule out the possibility that α and v would differ in the dilute and semidilute concentration regimes.

Dependence of Retardation on Particle Concentration. The retardation of particles in PA solutions was found to decrease with particle concentration (Figure 4). This decrease may be due to either a hydrodynamic interaction between single particles undergoing electrophoretic migration in the polymeric matrix or a particle aggregation. At concentrations close to the lowest particle concentration used ($\approx 2 \times 10^{-5}$ v/v), no aggregation of polystyrene latex spheres in aqueous polymer solutions is known to occur.[9,26,44−46] It could be suggested that, with increase in particle concentration, aggregates would start to form, with an effective aggregate size necessarily larger than that of a single particle. Since larger particles are shown to be less retarded by a polymer matrix, a progressive increase in the number of aggregates in the particle population undergoing electrophoretic migration will lead to an increase in mean electrophoretic mobility. It is expected that such progressive aggregation would give rise to a higher degree of size heterogeneity and, therefore, to result in increasing peak width. However, as demonstrated in Figure 5, a slight peak broadening with particle concentration, expressed by the relative peak width at half-height, $\Delta_{1/2}$, was exhibited only by PS-55 above $\Phi \approx 0.0002$, and peak width for PS-215 and -140 actually decreased. The decline for PS-215 is observed with Φ above $\Phi \approx 0.0002$ and that for PS-140 throughout the particle concentration range used. No steep transitions with particle concentration were observed with regard to both retardation and peak broadening (Figures 4 and 5) that would support a hypothesis of a cooperative change from a "nonaggregated" to an "aggregated" state. The attempt to directly investigate this matter by adding a nonionic detergent, Triton X-100, to particle suspensions failed since the presence of the detergent greatly influences the electrophoretic mobility of the particle in free buffer presumably due to a change in the "smoothness" of the particle surface,[47] which would render difficult any conclusion with regard to particle aggregation.

It is known that hydrodynamic interactions facilitate the translational motion of the particle in an assemblage of particles moving in an unconstrained ("infinitive") viscous medium if the only (or dominant) frictional force is the Stokes drag.[48] In the assemblage moving in a constrained space, the particle velocity may be decreased by hydrodynamic interactions due to the so-called "backflow" of the solvent.[49] The effect is known to be largely responsible for the concentration dependence of the sedimentation rate in colloidal systems. However, when the relatively diluted assemblage of, at the scale of κR, large particles undergoes electrophoretic migration in a viscous medium, the long-range hydrodynamic interactions are effectively screened due to electroosmotic slipping of fluid. Both mechanisms, facilitation of migration within an assemblage and enhanced resistance to migration due to "backflow", do not seem to be operative. Yet, solutions of polymers, especially in the entangled state, may be hardly considered as a pure viscous medium but rather represent a viscoelastic one.[21] Thus, once perturbed by passage of a particle, the medium will respond to the passage of the following (or neighboring) particle with a changed resistance depending on particle velocities, the average distance between particles in the assemblage, and the time required by the polymer network to restore the local equilibrium.

Irrespective of the source of the dependence of retardation in PA solutions on particle concentration, the rate of that dependence appears constant for different particles. Thus, at any given particle concentration within the range studied (Figure 4 and Table 1), the ratios between retardation and particle size appear to be the same. Therefore, one may assume that electrophoretic mobilities of particles within assemblages at a finite particle concentration may be employed to study the retardation of single particles by the polymeric matrix, at least qualitatively, despite the observed particle concentration dependence.

Dependence of Microviscosity on the Translational Motion Velocity of the Particle. It was found that the retardation of electrophoretic migration of the particle by PA solutions depends on the applied electric field strength (Figures 6 and 7). This, as was demonstrated, is not a result of Joule heating. Thus, for a given particle, the resistance of that medium to a translational motion of the particle seems to be a function of the rate of such motion. For the purposes of discussion, the

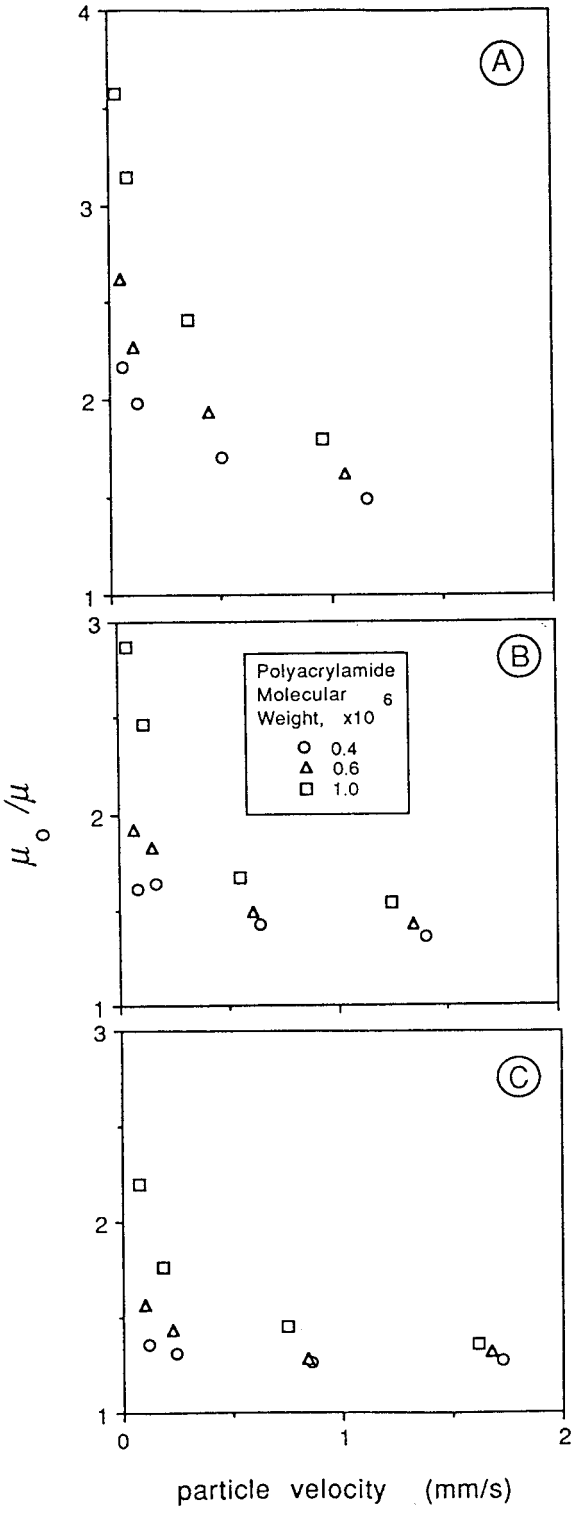

Figure 10. Microviscosity (μ_0/μ) of 1% solutions of polyacrylamide of different molecular weight vs translational velocity of the particle. Polystyrene latex spheres of 55 (panel A), 140 (panel B), and 215 nm (panel C) radius. Particle concentration and CZE conditions as in Figure 1 except for the electric field strength.

resistance of the medium, expressed as μ_0/μ, was plotted against the measured particle velocity, $v = \mu E$, at PA concentrations both below and above the polymer chain overlap threshold, c^* (Figures 9 and 10).

The values of microviscosity, μ_0/μ (eq 2), in Figures 9 and 10 are well below the corresponding values of macroviscosity for the PA-1 (Figure 2), PA-0.4, and PA-0.6 solutions. In the latter cases, the values of zero shear relative viscosity, η/η_0, at 1% PA concentration were found to equal 3.9 and 5.8, respectively. Yet, the values of μ_0/μ are particle velocity dependent and possibly may correspond to values of macroscopic viscosity at finite shear rates. The intriguing question is therefore what values of μ_0/μ are reached in the limit when the velocity of the translational motion of the particle approaches zero. In the range of electric field strengths compatible with capillary electrophoresis, the dependence of μ_0/μ on v is strong and obviously nonlinear for all particles in the PA-1 solution. However, the dependence is weakening for PS-140 and PS-215 in the PA-0.4 solution (Figure 10), thus allowing one to make a linear extrapolation to zero particle velocity. The extrapolation gives values of μ_0/μ in the limit of $v \rightarrow 0$ as 1.6 for PS-140 (Figure 10B) and 1.3 for PS-215 (Figure 10C), which are well below the viscometrically measured value of $\eta/\eta_0 = 3.9$ for zero shear viscosity in 1% PA-0.4 solutions. Generalizing this result, one may assume that values of μ_0/μ in Figures 9 and 10 do represent microscopic viscosity of polymer solutions for all sizes of PA used.

At the PA concentration of 0.008 gg^{-1} (Figure 9), the ratio of R/ξ increases with the radius of particles in the order of 7, 18, and 27. Thus, at the scale of R/ξ, the polymer solution definitely seems not to be a "continuum" for the smallest particles but to approach it for the largest. In any case, the penetration of these particles into the network must be accompanied by displacing polymer chains from the particle's path, and their resistance to such displacement may be a major cause of particle retardation. The displacement can occur due to either physical collisions of the polymer chains with the particle surface or to hydrodynamic interactions, or both. The hydrodynamic interaction between the chains and large (at the scale of κR) particles undergoing an electrophoretic migration can have a specific feature. In the submicron size range, particle radius is known to greatly exceed the thickness of the electric double layer (EDL) in most electrophoretic buffers. At an ionic strength of TB buffer equal to 0.0047,[1] κ^{-1} assumes a value of 4.4 nm,[12] which is sufficiently lower than the radius of the smallest polystyrene latex sphere used. Thus, for the particles under study, the long-range hydrodynamic interactions are screened by electroosmotic slipping, and the drag derives from the viscous friction within the EDL. Figuratively speaking, the EDL works as a tunnel to pump fluid from the front of the advancing particle. When polymer segments are present within the EDL, they will be entrained by the solvent motion that drags them along the particle surface. In turn, their motion would be translated to the chains. Since the size of submicron particles usually exceed R_g (for PA-1, $R_g = 44$ nm $< R$ of all particles under study), the displacement of polymer chains will occur over a distance longer than the characteristic size of polymer coils. In the entangled solution, it will inevitably result in a shear-like deformation of the network in the vicinity of the particle surface.

The shear deformation of a polymer network under laminar flow is well-known to decrease the macroscopic viscosity of entangled polymer solutions (known also as shear viscosity).[21,22,50] The decrease is believed to predominantly result from a decline in the entanglement density. The extent of this decline, according to Graessley,[50] depends on the characteristic time required for

entanglement by Brownian motion, τ_G, in relation to the transit time τ_p, during which polymer coils approximate each other sufficiently to become entangled. The "entanglement time", τ_G, may be estimated by the tube renewal time,[15]

$$T_R = (6\pi\eta_0/k_BT)R_g^3(c/c^*)^{1.5} \quad (10)$$

Assuming $\tau_G \cong T_R$, the "entanglement time" for the PA-1 solution at concentration of 0.008 gg^{-1} may be calculated as ≈2 ms. The transit time, τ_p, may be estimated as a ratio between R_g and the difference in velocities of adjacent laminar layers. In the case in question, that difference may be taken to equal the particle velocity, v. Accordingly, one obtains values of τ_p ranging from 1 to 0.02 ms for particle velocities of 0.04 to 2 mm/s, respectively (Figure 9). Thus, the values of microviscosity in Figure 9 seem to correspond to transit times that are less or much less than the characteristic time for entanglement in the PA solution. It may be suggested that the observed decrease in the resistance of the medium with particle velocity is due to a decline in the entanglement density of the network in the vicinity of the particle surface.

At a PA-1 concentration of 0.002 gg^{-1}, which is below c^* (0.003 gg^{-1}), polymer coils do not form a continuous spatial network in solution. However, the concentration seems to be high enough for a formation of transient associations of coils due to their partial interpenetration. For a polymer chain engaged with another chain (or chains), the friction exerted by chain segments located within the EDL on the flow in the EDL (and, thus, on the particle) may be a function of a chain "disengagement−reengagement" time, an analogue of τ_G, and the transit time, τ_p. Thus, the dependence of microviscosity on particle velocity in the dilute concentration regime could qualitatively resemble that in the semidilute regime, though quantitatively it must differ. Indeed, as seen in Figure 9, the microviscosity declines with v at both concentrations above c^* and below it but much more steeply at concentrations above it.

The displacement of polymer chains away from the front of the advancing particle in the "shear-deformation-like" manner, due to interaction of the chains adjacent to the particle surface with the flow within the EDL, can facilitate the particle penetration into the polymer network and explain the observed electric field strength dependent decrease of particle mobility in terms of the well-known shear rate dependent resistance of polymer networks to the shear deformation. However, it seems impossible to arrive at a conclusion on the basis of presently available experimental data as to what extent and in which direction the physical collisions of polymer chains with the particle surface, if they should occur, contribute to the retardation of the particle by the polymeric matrix.

Dependence of Microviscosity on Particle Size. The most interesting finding, especially for electrophoretic size-dependent particle separations, is that the microviscosity of semidilute PA solutions exhibits a size-dependent decrease in the range of 55−215 nm particle radius (Figures 3, 9, and 10), in contrast to predictions of the theoretical models. In the dilute concentration regime, the experimental data do not allow one to derive any firm conclusions about the dependence of microviscosity on particle size (Figure 9), and thus, it will not be discussed in this section.

The decrease in retardation with particle size is superimposed on that with particle velocity (Figures 9 and 10). For PA-0.4, the dependence is seen to be weak and allows one to obtain by linear extrapolation values of μ_0/μ in the limit of "zero particle velocity". These values were 1.3 for PS-215 and 1.6 for PS-140. As seen from Figure 10A, the corresponding value for PS-55 may be expected to be higher. However, for the polymers of higher molecular weight, such evaluations of the available data do not seem possible.

It is interesting to compare the dependencies of microviscosity on particle size, obtained by methods other than the electrokinetic one, viz. by studying particle diffusion or sedimentation in polymer solutions. In the pioneering work of Laurent and Pietruszkiewicz,[51] the authors have found that sedimentation rates of polystyrene latex particles in hyaluronic acid solutions decrease monotonically with particle radius in the range of 44−132 nm and remain invariant up to $R = 182$ nm. Since the authors did not report values of solution viscosities, it is not clear whether the particle retardation was governed by micro- or macroscopic viscosity of the polymer solutions. It is also not clear how charge interactions, likely to exist in a system consisting of charged particles and flexible polyelectrolytes, can affect the size-dependent retardation. Thus, only reports concerning the transport of, at the scale of R/ξ, "large" particles in solutions of neutral polymers, mostly in the semidilute concentration regime, will be considered in the discussion below. The discussion will also be limited to cases in which microviscosity does not exceed macroscopic viscosity; $\eta_\mu > \eta$ is usually interpreted in terms of polymer adsorption on the particle surface. (A list of relevant reports may be found, for example, in ref 7.) Turner and Hallet[52] and Phillies et al.[44] have studied the diffusion of polystyrene latex spheres ranging in size from 50 to 125 nm and from 20 to 640 nm radius, respectively, in aqueous solutions of dextran. These authors have found a decrease in the diffusion coefficient of the sphere with polymer concentration which is independent of particle radius. Yet, they have also found that values of viscosity obtained from particle diffusion in dextran solutions match those measured viscometrically.[44,52] Diffusion of polystyrene particles in aqueous solutions of PEG in the presence of Triton X-100 (to prevent PEG adsorption on the particle surface) was studied by Ullmann et al.[45] The results of those authors show that, when a significant decrease in solution viscosity estimated from the diffusion data (microviscosity) compared to that obtained viscometrically was observed, the microviscosity decreased with particle size in the range of 26−327 nm radius. However, in aqueous solutions of a semiflexible polymer, hydroxypropylcellulose, containing additionally a detergent, the opposite dependence was observed: microviscosity calculated accorging to the Stokes−Einstein law from translational diffusion coefficients of polystyrene latex spheres of 60−175 nm radius increased with sphere size.[46] Gold et al.[7] have studied the diffusion of polystyrene latex spheres of 152 and 208 nm radius through solutions of rigid rodlike polymer, poly(γ-benzyl-L-glutamate), of two different lengths in organic solvent (dimethylformamide). Microviscosity of solutions of the longer polymer was found to be much less that their macroscopic viscosity for both particles and the difference increased with particle size.

The data available from the literature do not allow a firm conclusion as to the dependence of microviscosity of semidilute solutions on the size of microparticles. Nonetheless, they show that the decrease of microviscosity with particle size is quite possible. It may be therefore assumed that, at a given velocity of particle migration, the observed decline in retardation with particle size not only results from differences in the network deformation at the scale of R/ξ or R/R_g but also reflects more fundamental interactions between submicron particles and polymer chains in the network. With an approach of the velocity of translational motion of the particle to a value of zero, such interactions may predominate.

Microviscosity and Polymer Depletion Layer. The theoretical description for microviscosity due to interface phenomena was first proposed by Donath and co-workers[53] in order to explain the largely increased electrophoretic mobility of particles compared to that expected according to eq 1. Such "enhanced" mobility was observed for cells, membrane vesicles, and polystyrene latex particles subjected to electrophoresis at relatively low field strengths (5−10 V/cm) in dilute solutions of dextran or PEG.[11,14,54−57] The theoretical evaluation has shown that, in the Smoluchowski limit ($R \gg \kappa^{-1}$), where all drag derives from the viscous friction within the EDL, the existence of a region with decreased density of polymer segments in the vicinity of the particle surface could result in a decline of the viscous friction imposed on the particle and, thus, in a higher electrophoretic mobility than that expected from the bulk solution viscosity.[53]

The region of polymer segment density decreasing in the direction toward a barrier, the so-called "depletion layer", is known to form near the interface between a solution of nonadsorbing polymers and solid surfaces. Its existence near flat static barriers was demonstrated both experimentally and theoretically in a number of reports (refs 19, 20, 58, and 59 and also references therein). Even in the absence of an enthalpic repulsive interaction like a polymer/surface incompatibility or electrostatic repulsion between polyelectrolytes and charged surfaces, the depletion layer can be formed due to the loss of configurational entropy of the polymer coils as a consequence of the steric restriction on the number of possible polymer chain configurations near the barrier. For the entropic repulsion, the depletion layer thickness equals the screening length, ξ, in the semidilute regime and is $\approx R_g$ of the polymer in the dilute regime. When unfavorable interactions between polymer segments and the barrier take place, the depletion layer thickness is expected to increase compared to that due to the entropic effect only.[19,20,58,59]

By using nuclear magnetic resonance, Cosgrove et al.[60] have shown the existence of a depletion layer of over 85 nm thickness around silica spheres of 116 nm diameter, diffusing through a semidilute aqueous solution of sodium poly(styrenesulfonate) (concentration = 7.8%, $M_r = 780\,000$). Such an extended depletion layer is thought to result mostly from the electrostatic repulsion between poly(styrenesulfonate) chains and the silica surface. This is the only experimental study that directly demonstrates the presence of a depletion layer around a colloidal particle in motion in a semidilute polymer solution. However, the formation of a depletion layer around particles performing Brownian motion is supported by the phenomena of particle flocculation in colloidal suspensions upon addition of nonadsorbing polymers which has been known for 60 years.[61] Such polymer-induced flocculation is attributed to depletion layers surrounding the colloidal particles.[19,20,58,59,61] The study of Arnold et al.[55] also strongly supports the idea that a depletion layer, at least in dilute polymer solutions, can form around particles that perform translational motion like electrophoretic migration. These authors have demonstrated, by applying fluorescence and electron spin resonance spectroscopy, that the surface potential of liposomes was not changed by the presence of PEG and, thus, cannot account for the observed electrophoretic mobility increase.[55]

Recently, the concept of depletion layer was employed by Gold et al.[7] to account for the "enhanced" diffusion of latex microspheres in semidilute solutions of polymers. These authors suggested that if a depletion layer exists locally around the spheres, the microviscosity experienced by the spheres will be smaller than the macroscopic viscosity. This hypothesis assumes that the depletion layer continually relocates as the sphere diffuses; thus, the sphere will always be locally moving in a solvent-rich space, exhibiting diffusion coefficients exceeding those predicted by the Stokes−Einstein equation, $D_{sphere} = k_B T/6\pi\eta R$. The depletion layer relocation implies that the rearrangement of the polymer network in the region around the sphere, which may be estimated by the tube renewal time, T_R (eq 10), occurs quickly at the scale of a characteristic time of particle diffusive motion.[7]

It may be assumed that the electrophoretic migration of latex particles under study in the semidilute PA solutions is also accompanied by formation and relocation of a depletion layer around the particles. When particle migration rates are low enough to allow the depletion layer to relocate due to network rearrangements, the "shearlike" polymer network deformation in the vicinity of the particle surface does not affect viscosity since entanglements are restored by Brownian motion of the chains and their density is not changed. However, the density of polymer segments present within the EDL is less than that in the bulk solution. As a result, viscous friction within the EDL which is responsible for particle retardation would be less than that expected from solution bulk viscosity. With an increase in particle velocity, at some point, the relocation of the depletion layer will fail since the network will not have time to adjust itself to the particle motion. Under those circumstances, an increase of microscopic viscosity and its approach to macroviscosity may be expected. Yet, at the same time, the entanglement density in the vicinity of particle surface has to start declining due to the "shearlike" deformation of the polymer network, which decreases the network resistance to the translational motion of the particle. It occurs since both "entanglement density restoration" and "polymer depletion layer relocation" are the result of the Brownian motion of the chains and depend on the same time parameter. The overall result of the competition between these opposite processes appears to be a decline in solution microviscosity with particle velocity (Figures 9 and 10). It cannot be ruled out that at the highest values of particle velocity the microviscosity will approach macroviscosity at some finite shear rate.

The theoretical calculations for depletion layers around objects of an arbitrary shape are usually based on the

assumption that the screening length, ξ, or polymer coil size, R_g, is much less that the characteristic size of those objects.[19,59] That assumption represents an approximation to an interface between a flat barrier and a polymer solution. How the depletion layer would form, if the radius of surface curvature does not greatly exceed the screening length or the polymer radius of gyration, is still an open question to our knowledge. At least in the case of the pure entropic interaction, the depletion layer would not form if a characteristic size of the object is commensurate with the size of the polymer network mesh. Hence, there has to be a transition region, at the scale of ξ/R, where a progressive formation of the depletion layer occurs around a spherical particle in semidilute solution of nonadsorbing polymers. It may be suggested that the observed decrease of microviscosity with particle size in the submicron size range reflects, in fact, the formation of a polymer depletion layer with increasing R at a given ξ.

Conclusions

The electrophoretic migration of highly cross-linked carboxylated PS spheres, in the submicron size range, through solutions of linear flexible neutral polymer, polyacrylamide, was studied by employing capillary zone electrophoresis. The particle retardation by the polymeric matrix was found to decrease with both particle radius and applied electric field strength. The solution viscosity derived from electrophoretic mobilities according to the Henry equation was well below zero shear viscosity measured viscometrically, even for a PA of M_r 4×10^5 and particles of 215 nm radius where no appreciable field strength dependence was observed. These findings were interpreted in terms of (i) a local shearlike deformation of the polymer network upon particle passage, resulting in decrease with translational velocity of the particle of the network entanglement density and, thus, a network resistance to particle penetration; and (ii) the progressive formation with particle radius, at the scale of R/ξ, of a polymer depletion layer near the particle surface that facilitates the electrophoretic migration of the particle in the polymer solution.

References and Notes

(1) Chrambach, A. *The Practice of Quantitative Gel Electrophoresis*; VCH: Weinheim, 1985.
(2) Viovy, J.-L.; Heller, C. In *Capillary Electrophoresis in Analytical Biotechnology*, Righetti, P.-G., Ed.; CRC Press: Boca Raton, FL, 1996; p 478.
(3) Quesada, M. A. *Curr. Opin. Biotechnol.* **1997**, *8*, 82.
(4) Chrambach, A.; Chen, N. *Electrophoresis* **1998**, *19*, 1279.
(5) Grossman, P. D. In *Capillary Electrophoresis*; Grossman, P. D., Colburn, J. C., Eds.; Academic Press: San Diego, CA, 1992; p 215.
(6) Radko, S. P.; Chrambach, A. *J. Chromatogr. B* **1999**, *722*, 1.
(7) Gold, D.; Onyenemezu, C.; Miller, W. G. *Macromolecules* **1996**, *29*, 5700, 5710.
(8) Langevin, D.; Rondelez, F. *Polymer* **1978**, *19*, 875.
(9) Nehme, O. A.; Johnson, P.; Donald, A. M. *Macromolecules* **1989**, *22*, 4326.
(10) Price, C. A. *Centrifugation in Density Gradients*, Academic Press: New York, 1892; p 264.
(11) Krabi, A.; Donath, E. *Colloids Surf. A* **1994**, *92*, 175.
(12) Hunter, R. J. *Zeta Potential in Colloid Science: Principles and Applications*; Academic Press: New York, 1981; Vol. 46, p 69.
(13) Dukhin, S. S.; Derjaguin, B. V. *Electrokinetic Phenomena In Surface and Colloid Science;* Matijevic, E., Ed.; John Wiley & Sons: New York, 1974; Vol. 7.
(14) Brooks, D. E.; Seaman, G. V. F. *J. Colloid Interface Sci.* **1973**, *43*, 670.
(15) De Gennes, P. G. *Macromolecules* **1976**, *9*, 587, 594.
(16) Langevin, D.; Rondelez, F. *Polymer* **1978**, *14*, 875.
(17) Lin, T.-H.; Philles, G. D. J. *J. Phys. Chem.* **1982**, *86*, 4073.
(18) Lin, T.-H.; Philles, G. D. J. *J. Colloid Interface Sci.* **1984**, *100*, 82.
(19) Joanny, J. F.; Leibler, L.; De Gennes, P. G. *J. Polym. Sci., Polym. Phys.* **1979**, *17*, 1073.
(20) Ausserre, D.; Hervet, H.; Rondelez, F. *Macromolecules* **1986**, *19*, 85.
(21) Ferry, J. D. *Viscoeleastic Properties of Polymers;* John Wiley & Sons: New York, 1980; p 29.
(22) Bohdanecky, M.; Kovar, J. *Viscosity of Polymer Solutions*; Elsevier Scientific: New York, 1982; Vol. 23, p 220.
(23) Hjerten, S. *J. Chromatogr.* **1985**, *347*, 191.
(24) Radko, S. P.; Garner, M. M.; Caiafa, G.; Chrambach, A. *Anal. Biochem.* **1994**, *223*, 981.
(25) Molyneux, P. *Water-Soluble Synthetic Polymers: Properties and Behavior* CRC Press: Boca Raton, FL, 1983; Vol. 1, p 84.
(26) Brown, W.; Rymdén, R. *Macromolecules* **1987**, *20*, 2867.
(27) Phillies, G. D. J.; Brown, W.; Zhou, P. *Macromolecules* **1992**, *25*, 4948.
(28) Broseta, D.; Leibler, L.; Lapp, A.; Strazielle, C. *Europhys. Lett.* **1986**, *2*, 733.
(29) Grossmann, P. D.; Soane, D. S. *Biopolymers* **1991**, *31*, 1221.
(30) Viovy, J.-L.; Duke, T. *Electrophoresis* **1993**, *14*, 322.
(31) Rodbard, D.; Chrambach, A. *Proc. Natl. Acad. Sci. U.S.A.* **1970**, *65*, 970.
(32) Ogston, A. G.; Preston, P. N.; Wells, J. D. *Proc. R. Soc. London, A* **1973**, *333*, 297.
(33) Altenberger, A. R.; Tirrel, M. *J. Chem. Phys.* **1984**, *80*, 2208.
(34) Cukier, R. I. *Macromolecules* **1984**, *17*, 252.
(35) Ogston, A. G. *Trans. Faraday Soc.* **1958**, *54*, 1754.
(36) Giddings, J. C.; Kucera, E.; Russel, C. P.; Myers, M. N. *J. Phys. Chem.* **1968**, *72*, 4397.
(37) Slater, G. W.; Treurniet, J. R. *J. Chromatogr.* **1997**, *772*, 39.
(38) Radko, S. P.; Chrambach, A. *Biopolymers* **1997**, *42*, 183.
(39) Phiilies, G. D. J. *Biopolymers* **1985**, *24*, 379.
(40) Radko, S. P.; Chrambach, A. *J. Phys. Chem.* **1996**, *100*, 19461.
(41) Laurent, T. C.; Persson, H. *Biochim. Biophys. Acta* **1964**, *83*, 141.
(42) Radko, S. P.; Chrambach, A. *Electrophoresis* **1996**, *17*, 1094.
(43) Wu, C.; Quesada, M. A.; Schneider, D. K.; Farinato, R.; Studier, F. W.; Chu, B. *Electrophoresis* **1996**, *17*, 1103.
(44) Phillies, G. D. J.; Gong, J.; Li, L.; Rau, A.; Zhang, K.; Yu, L.-P.; Rollings, J. *J. Phys. Chem.* **1989**, *93*, 6219.
(45) Ullmann, G. S.; Ullmann, K.; Linder, R. M.; Phillies, G. D. J. *J. Phys. Chem.* **1985**, *89*, 692.
(46) Yang, T.; Jamieson, A. M. *J. Colloid Interface Sci.* **1988**, *126*, 220.
(47) Ohshima, H. *Adv. Colloid Interface Sci.* **1995**, *62*, 189.
(48) Happel, J.; Brenner, H. *Low Reynolds Number Hydrodynamics*; Prentice-Hall: Englewood Cliffs, NJ, 1965; p 235.
(49) Enoksson, B. *Nature* **1948**, *161*, 9341.
(50) Graessley, W. W. *Adv. Polym. Sci.* **1974**, *16*, 1.
(51) Laurent, T. C.; Pietruszkiewicz, A. *Biochim. Biophys. Acta* **1961**, *49*, 258.
(52) Turner, D. N.; Hallett, F. R. *Biochim. Biophys. Acta* **1976**, *451*, 305.
(53) Donath, E.; Kuzmin, P.; Krabi, A.; Voigt, A. *Colloid Polym. Sci.* **1993**, *271*, 1, 930.
(54) Snabre, P.; Mills, P. *Colloid Polym. Sci.* **1985**, *263*, 494.
(55) Arnold, K.; Zschoerning, O.; Barthel, D.; Herold, W. *Biochim. Biophys. Acta* **1990**, *1022*, 303.
(56) Donath, E.; Krabi, A.; Allan, G.; Vincent, B. *Langmuir* **1996**, *12*, 3425.
(57) Krabi, A.; Allan, G.; Donath, E.; Vincent, B. *Colloids Surf.* **1997**, *122*, 33.
(58) Rondelez, F.; Ausserre, D.; Hervet, H. *Annu. Rev. Phys. Chem.* **1987**, *38*, 317.
(59) Fleer, G. J.; Cohen Stuart, M. A.; Scheutjens, J. H. H. M.; Cosgrove, T.; Vincent, B. *Polymers at Interfaces*; Chapman and Hall: London, 1993.
(60) Cosgrove, T.; Obey, T. M.; Ryan, K. *Colloids Surf.* **1992**, *65*, 1.
(61) Vrij, A. *Pure Appl. Chem.* **1976**, *48*, 471.

MA9814447